

Recursive Gabor Filtering

Ian T. Young, *Senior Member, IEEE*, Lucas J. van Vliet, and Michael van Ginkel

Abstract—In this paper, we present a stable, recursive algorithm for the Gabor filter that achieves—to within a multiplicative constant—the fastest possible implementation. For a signal consisting of N samples, our implementation requires $O(N)$ multiply-and-add (MADD) operations, that is, the number of computations per input sample is constant. Further, the complexity is independent of the values of σ and ω in the Gabor kernel, and the coefficients of the recursive equation have a simple, closed-form solution given σ and ω . Our implementation admits not only a “forward” Gabor filter but an inverse filter that is also $O(N)$ complexity.

Index Terms—Gabor filtering, Gabor wavelets, IIR filters, multidimensional filtering, recursive filtering.

I. INTRODUCTION—WHY GABOR FILTERING?

WHILE operators that focus on global information are essential to describing a variety of physical *systems*, operators that focus on local information are essential to analyzing physical *signals*. For example, linear, time-invariant (or shift-invariant) systems are usually analyzed with Fourier or Laplace transforms, which are global operations, but as the examples in Fig. 1 show, the information in a signal is usually local.

Although there are many approaches to processing signals in such a way as to examine the local character of structure, the Gabor filter has a number of elegant properties that make it highly suitable for this purpose. The complex, one-dimensional (1-D) Gabor filter is given by [1]

$$g(t|\sigma, \omega) = \underbrace{\frac{1}{\sqrt{2\pi}\sigma} e^{-t^2/2\sigma^2}}_{\text{Gaussian envelope}} \underbrace{e^{j\omega t}}_{\text{Modulation term}}. \quad (1)$$

It is clear that the Gabor filter is the *modulation* of a Gaussian kernel by the complex term $e^{j\omega t}$. The use of the complex term means that we will be using complex arithmetic in all calculations.

To examine local structures, we seek a filter width in *time* (or space) that is narrow. To obtain good frequency resolution, we seek a filter width in *frequency* that is similarly narrow. The Gaussian envelope in (1) achieves the smallest possible time-bandwidth product and, thus, allows us to perform “local” spectral analysis [1], [2]. In the sense of simultaneous time and

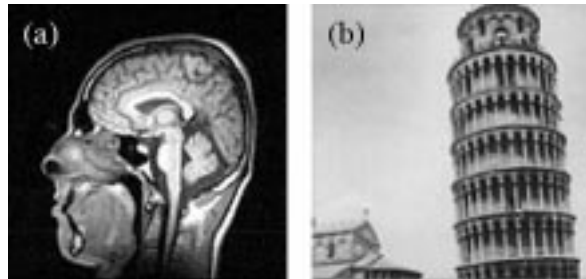


Fig. 1. (a) MRI image revealing (local) anatomical structures. (b) Leaning tower of Pisa.

frequency selectivity, the Gabor filter is, therefore, an optimum choice.

Further, a number of authors have pointed out the close relationship between the neurophysiological processing of visual and tactile stimuli and families of 1-D and two-dimensional (2-D) Gabor filters [3]–[8]. In particular, Baker *et al.*, in referring to their observation of Gabor-type oscillations in neurophysiological measurements [8, Fig. 9, p. 238], writes “*these oscillations are a pervasive feature of the nervous system.*”

The possibilities for fast implementation of the Gabor time-frequency spectrum (spectrogram) have been examined by [9]–[11]. To our knowledge, the fastest algorithms that have been described are in Qiu [11] and, for a signal consisting of N samples, the time–frequency spectrum has complexity $O(N \bullet \log N)$. Our implementation of an IIR Gabor filter (as opposed to a complete determination of a Gabor spectrogram) is based on our recursive Gaussian implementation. Because of this, we summarize the salient aspects of the Gaussian procedure.

II. REVIEW OF THE RECURSIVE GAUSSIAN

In two previous papers, we have developed [12] and refined [13] a method to implement the convolution of signals with Gaussian kernels through the use of two recursive filters of the form:

forward (n increasing): [shown in (2) at the bottom of next the page] and *backward* (n decreasing): [shown in (3) at the bottom of the next page].

Note that in this implementation, shown in Fig. 2, the forward filter has an infinite impulse response (IIR), which we can call $h[n]$, and the backward filter has the infinite impulse response $h[-n]$.

The concatenation of the two filters, as given in (2) and (3), leads to a total filter $p[n] = h[n] \otimes h[-n]$, whose Fourier transforms are related by $P(\Omega) = |H(\Omega)|^2$. In other words, the resulting filter $p[n]$ is zero phase.

Manuscript received May 30, 2001; revised June 26, 2002. This work was supported in part by the Rolling Grants program of the Dutch Foundation for Fundamental Research in Matter (FOM) and the Delft Universiteitsfonds. The associate editor coordinating the review of this paper and approving it for publication was Dr. Paulo J. S. G. Ferreira.

The authors are with the Pattern Recognition Group, Department of Applied Physics, Delft University of Technology, Delft, The Netherlands (e-mail: young@ph.tn.tudelft.nl; lucas@ph.tn.tudelft.nl; michael@ph.tn.tudelft.nl).

Digital Object Identifier 10.1109/TSP.2002.804095.

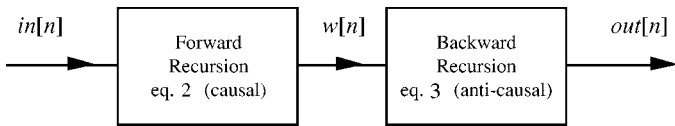


Fig. 2. Gaussian filter as concatenation of two recursive filters.

We approach the Gaussian filtering through the complex frequency domain and use a rational approximation to the Gaussian spectrum given by [12] and [14, Eq. 26.2.20]:

$$G_q(s) = \frac{a_0}{a_0 - (a_2q^2)s^2 + (a_4q^4)s^4 - (a_6q^6)s^6} \quad (4)$$

where

$$\begin{aligned} a_0 &= 2.490\ 895 & a_2 &= 1.466\ 003 \\ a_4 &= -0.024\ 393 & a_6 &= 0.178\ 257. \end{aligned} \quad (5)$$

Note our use of q instead of σ , which is an issue that will be discussed later. The sixth-order polynomial in the denominator of $G_q(s)$ has six roots that, due to the special structure of the polynomial, only even powers of s , can be written as shown in (7), where

$$m_0 = 1.166\ 80 \quad m_1 = 1.107\ 83 \quad m_2 = 1.405\ 86. \quad (6)$$

These three values $\mathbf{m} = \{m_0, m_1, m_2\}$ are central to the Gabor filter as well. They are solely determined by the values of $\mathbf{a} = \{a_0, a_2, a_4, a_6\}$ and if another choice of \mathbf{a} is made—for example, to optimize the Gaussian fit with another criterion—then the values of \mathbf{m} will change as well.

The expression $G_q(s)$ is then factored into the *product* of two terms $G_q(s) = G_L(s) \bullet G_R(s)$: $G_L(s)$ with poles in the left-half plane and $G_R(s)$ with poles in the right-half plane

$$G_q(s) = \frac{a_0}{(qs + m_0)(qs + m_1 + jm_2)(qs + m_1 - jm_2)} \times \frac{1}{(qs - m_0)(qs - m_1 - jm_2)(qs - m_1 + jm_2)}. \quad (7)$$

For reasons discussed in [12], we use the backward difference technique and the forward difference technique [2] to transform the two, stable, analog filters characterized by $G_L(s)$ and $G_R(s)$ into two, stable, digital filters $H_+(z)$ and $H_-(z)$. The backward technique is used to transform $G_L(s)$ into $H_+(z)$, and the forward technique is used to transform $G_R(s)$ into $H_-(z)$. These

filters then have z -transforms given by

$$H_+(z) = \frac{1}{b_0 + b_1z^{-1} + b_2z^{-2} + b_3z^{-3}} \quad (8)$$

$$H_-(z) = \frac{B}{b_0 + b_1z^1 + b_2z^2 + b_3z^3}. \quad (9)$$

Algebraic manipulation of the various terms using Mathematica [15] yields

$$\begin{aligned} b_0 &= 1 & \text{scale} &= (m_0 + q)(m_1^2 + m_2^2 + 2m_1q + q^2) \\ b_1 &= -q \frac{(2m_0m_1 + m_1^2 + m_2^2 + (2m_0 + 4m_1)q + 3q^2)}{\text{scale}} \\ b_2 &= q^2 \frac{(m_0 + 2m_1 + 3q)}{\text{scale}} \\ b_3 &= -\frac{q^3}{\text{scale}}. \end{aligned} \quad (10)$$

The five coefficients $\{b_0, b_1, b_2, b_3, \text{scale}\}$ are real and are functions of just four numbers $\{m_0, m_1, m_2, q\}$, as given in (10). The first three of these are given in (6). The last number q represents the value that must be used in $\{(8) \text{ and } (9)\}$ to achieve a desired standard deviation σ . Using a new analytical formula that is a significant improvement to the empirical one presented in [12], the relationship between q and σ for recursive Gaussian filtering is given by

$$q(\sigma) = 1.315\ 64 \bullet \left(\sqrt{1 + 0.490\ 811 \bullet \sigma^2} - 1 \right) \quad \sigma \geq 1.0. \quad (11)$$

The details of the development of this formula are given in the Appendix . For $\sigma < 1.0$, the Gaussian envelope in (1) is too narrow and, consequently, undersampled and, in general, to be avoided. The accuracy, speed, and guaranteed stability of this recursive Gaussian implementation are discussed extensively in [12] and [13], as is the choice of optimal values for the coefficient set \mathbf{a} from (5).

III. GABOR ALGORITHM

A. From Gauss to Gabor

Our recursive Gabor filter uses a combination of our recursive Gaussian implementation plus a well-known property that relates modulation at a frequency Ω_o in the (discrete) time domain and shifting in the frequency domain. To be specific, if the signal $h[n]$ has z -transform $H(z)$, then from [2, pp 650–651], we have

$$Z \{ e^{j\Omega_o n} h[n] \} = H(e^{-j\Omega_o} z). \quad (12)$$

$$w[n] = \frac{(in[n] - (b_1 \bullet w[n - 1] + b_2 \bullet w[n - 2] + b_3 \bullet w[n - 3]))}{b_0} \quad (2)$$

$$out[n] = \frac{(B \bullet w[n] - (b_1 \bullet out[n + 1] + b_2 \bullet out[n + 2] + b_3 \bullet out[n + 3]))}{b_0} \quad (3)$$

Note that the replacement of z with $e^{-j\Omega_o}z$ represents a rotation of angle Ω_o around the point $z = (0, 0)$ in the complex z -plane. The direct consequence of this is that the Gaussian filter pair $H_+(z)$ and $H_-(z)$ become the Gabor filter pair $B_+(z)$ and $B_-(z)$

$$B_+(z, \Omega_o) = \frac{1}{\sum_{k=0}^3 (b_k e^{jk\Omega_o} z^{-k})} = \frac{1}{P_+(z)} \quad (13)$$

$$B_-(z, \Omega_o) = \frac{B}{\sum_{k=0}^3 (b_k e^{-jk\Omega_o} z^k)} = \frac{1}{P_-(z)} \quad (14)$$

where $P_+(z)$ and $P_-(z)$ are polynomials in z . The Gabor filter transfer function $G(z)$ is thus given by

$$G(z) = B_+(z, \Omega_o)B_-(z, \Omega_o) = \frac{1}{P_+(z)P_-(z)}. \quad (15)$$

The coefficient of each term in z^k in $P_-(z)$ [see (14)] is just the complex conjugate of the term in z^{-k} in $P_+(z)$ [see (13)].

The resulting Gabor recursive equation pair is
forward (n increasing):

$$w[n] = \text{in}[n] - ((b_1 \bullet e^{j\Omega_o} \bullet w[n-1]) + (b_2 \bullet e^{j2\Omega_o} \bullet w[n-2]) + (b_3 \bullet e^{j3\Omega_o} \bullet w[n-3])) \quad (16)$$

backward (n decreasing):

$$\begin{aligned} \text{out}[n] = & B \bullet w[n] \\ & - ((b_1 \bullet e^{-j\Omega_o} \bullet \text{out}[n+1]) \\ & + (b_2 \bullet e^{-j2\Omega_o} \bullet \text{out}[n+2]) \\ & + (b_3 \bullet e^{-j3\Omega_o} \bullet \text{out}[n+3])) \end{aligned} \quad (17)$$

where

$$B = \left(\frac{m_0 (m_1^2 + m_2^2)}{\text{scale}} \right)^2. \quad (18)$$

B. Implementation Issues

The expression for q , which is described in (11), was derived for the Gaussian filter. For the Gabor filter, the problem is much more complex. A simple, closed-form solution as in (11) does not seem possible. Based on the approach we used in [12], we have performed a regression analysis on $\{q, \sigma\}$ to determine their relationship. This has led to the empirical result

$$q(\sigma) = \begin{cases} -0.2568 + 0.5784\sigma + 0.0561\sigma^2, & \sigma < 3.556 \\ 2.5091 + 0.9804(\sigma - 3.556), & \sigma \geq 3.556. \end{cases} \quad (19)$$

Further, let us assume that the 1-D signal that is to be filtered is of length N , that is, $n = 1, 2, \dots, N$. In the forward (causal) direction, it is important to use proper values for the first three values of (16). These are given by

$$\begin{aligned} w[1] = w[2] = w[3] \\ = \frac{\text{in}[1]}{(1 + b_1 \bullet e^{j\Omega_o} + b_2 \bullet e^{j2\Omega_o} + b_3 \bullet e^{j3\Omega_o})}. \end{aligned} \quad (20)$$

The recursion then starts at $n = 4$ and proceeds to $n = N$. In the backward (anti-causal) direction, it is equally important to use proper values for the “first” three values of (17). These are given by

$$\begin{aligned} \text{out}[N] = \text{out}[N-1] = \text{out}[N-2] \\ = \frac{B \bullet w[N]}{(1 + b_1 \bullet e^{-j\Omega_o} + b_2 \bullet e^{-j2\Omega_o} + b_3 \bullet e^{-j3\Omega_o})}. \end{aligned} \quad (21)$$

The recursion then starts with $n = N - 3$ and continues to $n = 1$.

Applying this algorithm to a simple impulse input to achieve the discrete time equivalent of (1) produces the impulse response $g[n|\sigma, \Omega]$ shown in Fig. 3 for several values of Ω and σ .

The last example in Fig. 3 shows an interesting effect. The total signal width is $N = 100$, and σ is 20.0. For the impulse response to be sufficiently small at the boundary of the signal, we usually require a Gaussian to be down by about 3σ . For purposes that will become clear later, we will require the Gaussian impulse response to be down by $\pi\sigma$. This must occur at both ends of the signal, that is, at $n = 1$ and $n = N$. This means that σ and N should satisfy the constraint $2\pi\sigma \leq N$. This constraint is not satisfied in the $\sigma = 20.0$ example, and that explains the truncated ends of the Gaussian.

Extending this argument to the frequency domain means that to avoid distortion of the frequency spectrum, we must have a σ such that the Gaussian spectrum has also decreased by the same amount at the maximum frequency $\Omega = \pi$. This implies that $\sigma \geq 1$. This translates into the constraint given in (11). Putting these two constraints together—the avoidance of spatial aliasing and spectral aliasing—leads to

$$1 \leq \sigma \leq \frac{N}{2\pi}. \quad (22)$$

C. Accuracy of Approximation

Although Fig. 3 and (22) give an indication of how the choice of σ can produce obvious distortions in the final result, it is also important to examine the error that occurs due to the recursive Gabor approximation itself. To do this, we use the error measures that were used for evaluation of the recursive Gaussian approximation: the maximum absolute error and the root-square error. These are defined as [12], [13]

$$\begin{aligned} \max_abs_err(\sigma, \Omega) &= \max_n \{ |\varepsilon[n|\sigma, \Omega]| \} \\ \text{root_square_err}(\sigma, \Omega) &= \sqrt{\sum_n |\varepsilon[n|\sigma, \Omega]|^2} \end{aligned} \quad (23)$$

where $\varepsilon[n|\sigma, \Omega]$ is the complex difference between the ideal Gabor impulse response $\text{gabor}[n|\sigma, \Omega]$ and the result of the recursive approximation $\text{out}[n|q(\sigma), \Omega]$ from (17). Thus, $\varepsilon[n|\sigma, \Omega] = \text{gabor}[n|\sigma, \Omega] - \text{out}[n|q(\sigma), \Omega]$. However

$$\text{gabor}[n|\sigma, \Omega] = \text{gauss}[n|\sigma] e^{j\Omega n} \quad (24)$$

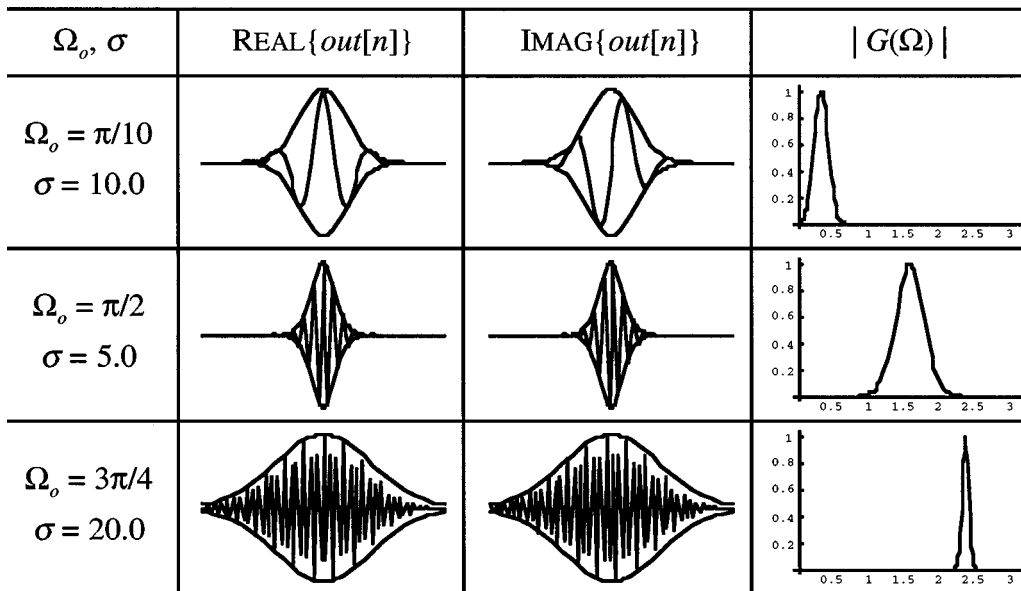


Fig. 3. Complex impulse response $g[n]$ and Fourier spectrum $G(\Omega)$ for various values of Ω_o and σ . Signal length is $N = 100$. Gaussian envelopes have been drawn for purposes of comparison.

where $\text{gabor}[\bullet]$ and $\text{gabor}[\bullet]$ are the true Gabor and Gauss filters, respectively, and

$$\text{out}[n|q, \Omega] = \text{out}_{\text{gauss}}[n|q]e^{j\Omega n} \quad (25)$$

where $\text{out}[\bullet]$ and $\text{out}_{\text{gauss}}[\bullet]$ are our recursive approximations to the Gabor and Gauss, respectively. The fact that this last result (25) can be factored is a direct consequence of our construction of the Gabor approximation as given in (12). Using these two results we see that

$$\begin{aligned} |\varepsilon[n|\sigma, \Omega]| &= |\text{gabor}[n|\sigma, \Omega] - \text{out}[n|q, \Omega]| \\ &= |\text{gauss}[n|\sigma]e^{j\Omega n} - \text{out}_{\text{gauss}}[n|q]e^{j\Omega n}| \\ &= |\text{gauss}[n|\sigma] - \text{out}_{\text{gauss}}[n|q]|. \end{aligned} \quad (26)$$

The last term is simply the error associated with the recursive Gaussian approximation: an error that was studied in [12]. Evaluation of these error measures over the range $1 \leq \sigma \leq 20$ yields the results shown in Fig. 4: a result that is independent of Ω .

D. Inverse Filtering

Our procedure also admits a direct implementation of the inverse filter. If the forward transform represented by (16) and (17) is given (in the z -domain) by the equation

$$\begin{aligned} \text{OUT}(z) &= G(z, \Omega_o)IN(z) \\ &= B_-(z, \Omega_o)(B_+(z, \Omega_o) \bullet IN(z)) \end{aligned} \quad (27)$$

then the inverse filter $\text{Inv}G(z)$ is simply:

$$\text{Inv}G(z) = \frac{1}{G(z, \Omega_o)} = \frac{1}{B_-(z, \Omega_o)B_+(z, \Omega_o)}. \quad (28)$$

The filters $B_+(z)$ and $B_-(z)$ are all-pole filters, which means that their inverses are all-zero filters that are nonrecursive and stable. The difference equations are given by

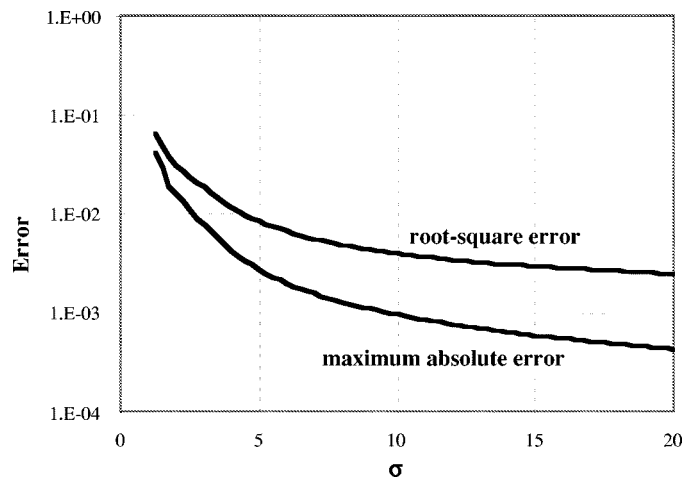


Fig. 4. Error measures as a function of σ and Ω . Both curves are independent of Ω .

forward (n increasing):

$$\begin{aligned} u[n] &= \text{out}[n] + b_1 \bullet e^{j\Omega_o} \bullet \text{out}[n-1] \\ &\quad + b_2 \bullet e^{j2\Omega_o} \bullet \text{out}[n-2] + b_3 \bullet e^{j3\Omega_o} \bullet \text{out}[n-3] \end{aligned} \quad (29)$$

backward (n decreasing): [see (30) at the bottom of the next page].

E. Computational Complexity

Use of this recursive Gabor implementation then becomes a matter of using the following ‘‘recipe’’:

- 1) Choose σ and Ω_o based on the desired goal of the filtering.
- 2) Use (19) to determine q .
- 3) Use (10) and (18) to determine the various coefficients.
- 4) Use (20) and (21) to initialize the procedure.
- 5) Apply the forward filter with (16).
- 6) Apply the backward filter with (17).

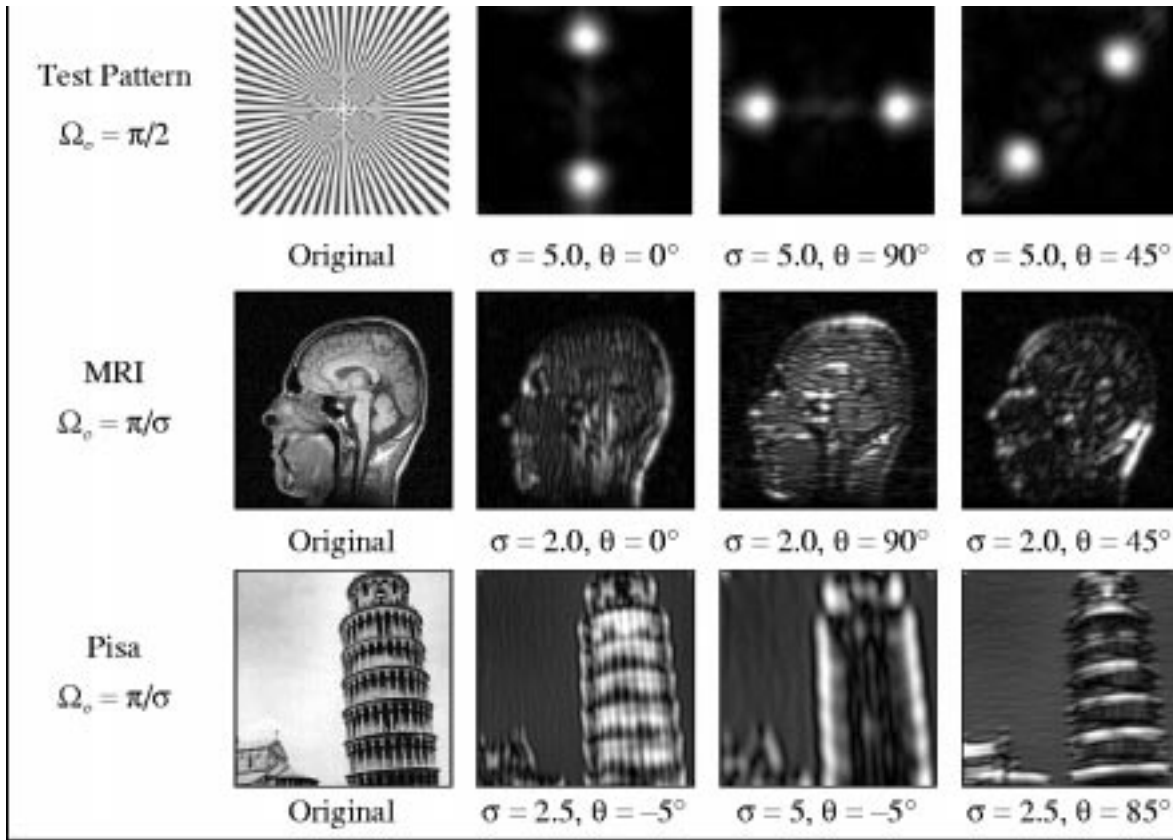


Fig. 5. Gabor filtering of a real image produces a complex result. We show here the absolute value of that complex result. The value of Ω_o in the last two rows is based on a neurophysiological model and is given by $\Omega_o = \pi/\sigma$.

As (16) and (17) require a total of seven complex multiplies and six complex additions for each output point, the complexity of the Gabor filtering algorithm for N input data points is $7 \bullet k \bullet N$, where k is the constant associated with one complex MADD. The complexity per input point is thus a constant $7 \bullet k$. This means that to within this multiplicative constant, this is the fastest possible implementation as every input point *must* be “visited” at least once. If we were to use an implementation based on an FFT for the Gabor filtering, which assumes that N is a composite number, then the complexity per input point would be $k' \bullet \log_2 N$. While this *could* be less than $7 \bullet k$, this would only be for trivially small values of N . For example, for $N = 2^4 = 16$, Gabor filtering with the recursive procedure is already faster than an FFT procedure.

F. Two-Dimensional Filtering

Gabor filtering is frequently used in multidimensional signal processing. By applying the recursive Gabor procedure previously described along each dimension of the signal, it is possible to implement the class of *separable* Gabor filters. We show in

Fig. 5 the effect on three images of Gabor filtering applied in several directions. The 2-D Gabor filter kernel is defined as

$$\begin{aligned}
 g(x, y; \sigma_x, \sigma_y, \Omega_x, \Omega_y) &= \frac{1}{2\pi\sigma_x\sigma_y} e^{-(1/2)(x^2/\sigma_x^2 + y^2/\sigma_y^2)} \\
 &\quad \times e^{j(\Omega_x x + \Omega_y y)} \\
 &= \frac{1}{\sqrt{2\pi}\sigma_x} e^{-(x^2/2\sigma_x^2)} e^{j\Omega_x x} \\
 &\quad \times \frac{1}{\sqrt{2\pi}\sigma_y} e^{-(y^2/2\sigma_y^2)} e^{j\Omega_y y}. \quad (31)
 \end{aligned}$$

In Fig. 5, we use $\sigma_x = \sigma_y = \sigma$. This filter can then be applied at various orientations θ through variation of the frequencies as $\Omega_x = \Omega_o \bullet \cos \theta$ and $\Omega_y = \Omega_o \bullet \sin \theta$. We also show in Fig. 5 the results of Gabor filtering for specific choices of Ω and σ for the images shown in Fig. 1. In the last two rows of these results, we have imposed a constraint suggested by Lee [7, eq. (10)] that $\sigma \bullet \Omega = \kappa$. As explained in his excellent paper, the inverse relationship between σ and Ω is based on neurophysiological data for the visual cortex. The exact choice of κ is not critical, and for the examples in Fig. 5, we have chosen $\kappa = \pi$. This brings

$$in[n] = \frac{(u[n] + (b_1 \bullet e^{-j\Omega_o} \bullet u[n+1]) + (b_2 \bullet e^{-j2\Omega_o} \bullet u[n+2]) + (b_3 \bullet e^{-j3\Omega_o} \bullet u[n+3]))}{B} \quad (30)$$

us to a consistent representation with respect to (22). Automatic contrast scaling has been applied to the resulting images.

IV. GABOR WAVELETS

With one addition, the technique described previously can be used to produce a Gabor wavelet representation of a signal. A requirement for a family of signals to be admissible as wavelets is that they have zero mean, that is, a dc component of zero [7, eq. (10)]. From the results shown in Fig. 3 as well as the form of (1), it is obvious that although the imaginary part of the Gabor impulse response $g[n]$ has zero mean because it is an odd function, the real part of $g[n]$ is even and does not have zero mean. The following well-known result gives us a mechanism to explicitly determine the value of the dc component

$$\begin{aligned} \mu_g &= G(z=1) = B_+(1, \Omega_o) B_-(1, \Omega_o) \\ &= \sum_{n=-\infty}^{n=+\infty} g[n] z^{-n} \Big|_{z=1} = \sum_{n=-\infty}^{n=+\infty} g[n]. \end{aligned} \quad (32)$$

The result is quite complicated but is presented here for the sake of completeness:

$$\mu_g = \frac{\text{Numerator}(m_0, m_1, m_2, q)}{\text{Denominator}(m_0, m_1, m_2, q)} \quad (33)$$

where

$$\begin{aligned} \text{Numerator}(m_0, m_1, m_2, q) &= (m_0 (m_1^2 + m_2^2))^2 \\ \text{Denominator}(m_0, m_1, m_2, q) &= (m_0^2 + 2m_0q + 2q^2 - 2q(m_0 + q) \cos(\Omega_o)) \\ &\quad \times (m_1^4 + 2m_1^2m_2^2 + m_2^4 + 4m_1^3q + 4m_1m_2^2q \\ &\quad + 10m_1^2q^2 + 2m_2^2q^2 + 12m_1q^3 + 6q^4 - 4q(m_1 + q) \\ &\quad \times (m_1^2 + m_2^2 + 2m_1q + 2q^2) \cos(\Omega_o) \\ &\quad + 2q^2 (m_1^2 + m_2^2 + 2m_1q + 2q^2) \cos(2\Omega_o)). \end{aligned} \quad (34)$$

For a specific set \mathbf{m} and specific choices for Ω_o and σ , the value of μ_g can be determined. For the example shown at the top of Fig. 3, where $\Omega_o = \pi/10$ and $\sigma = 10$, $\mu_g = 0.0280448$. By subtracting this value from the total transfer function $B_+(z) \bullet B_-(z)$ [7, eq. (14)], we create a new (Gabor wavelet) transfer function $W_g(z)$ whose value is zero for $z = 1$. This transfer function will have both zeroes and poles

$$\begin{aligned} W_g(z) &= G(z) - \mu_g = B_+(z, \Omega_o) B_-(z, \Omega_o) - \mu_g \\ &= \left(\frac{1}{P_+(z)} \right) \left(\frac{1}{P_-(z)} \right) - \mu_g \\ &= \frac{1 - \mu_g P_+(z) P_-(z)}{P_+(z) P_-(z)}. \end{aligned} \quad (35)$$

The actual implementation of (35) as a recursive filter requires an alternative approach. Each of the polynomials $P_+(z)$ and $P_-(z)$ is a third-order polynomial and, thus, has three complex

roots. The expression $1/(P_+P_-)$ can therefore be rewritten as a parallel operation instead of the series one illustrated in Fig. 2:

$$\begin{aligned} \frac{1}{P_+(z)P_-(z)} &= \underbrace{\left(\frac{\alpha_{+1}}{z^{-1} + z_{+1}} + \frac{\alpha_{+2}}{z^{-1} + z_{+2}} + \frac{\alpha_{+3}}{z^{-1} + z_{+3}} \right)}_{\text{forward recursion}} \\ &\quad + \underbrace{\left(\frac{\alpha_{-1}}{z + z_{-1}} + \frac{\alpha_{-2}}{z + z_{-2}} + \frac{\alpha_{-3}}{z + z_{-3}} \right)}_{\text{backward recursion}} \end{aligned} \quad (36)$$

where $\{z_{+1}, z_{+2}, z_{+3}\}$ are the roots of $P_+(z)$, and $\{z_{-1}, z_{-2}, z_{-3}\}$ are the roots of $P_-(z)$. The various α 's are constants that must be determined by standard partial fraction expansion techniques. The actual subtraction of μ_g need only be associated with one of the six terms, for example

$$\frac{\alpha_{-3}}{z + z_{-3}} - \mu_g = \frac{(\alpha_{-3} - \mu_g z_{-3}) - \mu_g z}{z + z_{-3}}. \quad (37)$$

The wavelet filtering from (35) can thus be implemented as six parallel operations that are then added together. If our purpose is wavelet analysis, then the presence of zeroes will not be a problem, but if our intent is to reconstruct the original signal from the wavelet representation, then the inverse technique involving recursive filtering described previously will not work due to the guaranteed *instability* of $(W_g(z))^{-1}$. We are currently exploring a recursive procedure for signal reconstruction from the wavelet representation that will avoid this problem.

V. CONCLUSIONS

This approach to Gabor filtering described here provides an accurate and fast algorithm that is appropriate when the values of σ and Ω are known. When a range of Ω 's must be investigated (as, for example, in a Gabor time-frequency spectrum), then the more general approach, such as that in [11], should be considered. As presented in Section III-C, the accuracy is the same as the results we achieved for recursive Gaussian filtering: results that are sufficient to the task. We will, however, continue to seek an analytical solution to replace the empirical result in (19). As shown in Section III-E, the computational complexity for N input samples is $O(N)$, which is faster than an FFT approach. In every case, the avoidance of aliasing requires a constraint on the choice of σ for a given signal length N , as given in (22): $1 \leq \sigma \leq N/2\pi$.

The algorithm can be applied to multidimensional signals when one is interested in the class of separable filters such as $g[n, m\{\bullet\}] = g[n\{\bullet\}]g[m\{\bullet\}]$, as shown in (31). While this limits the domain of applicability, there are still sufficient examples that fall into this category as to warrant its description. Examples include the detection of lines and edges in man-made objects.

We have developed an inverse to the Gabor filter as well as an algorithm for Gabor wavelet representation. It should be apparent that we do not (as yet) have a mechanism for producing a recursion based on either σ or Ω . This means that a signal must be filtered for each *and every* value of (σ, Ω) to produce the desired result. In certain application domains, however, when a relationship, such as $\sigma \bullet \Omega = \kappa$, is known, an evaluation over

all Ω 's is unnecessary when a search over the desired range of σ 's is performed.

APPENDIX

There is a well-known relationship between the calculation of the second moment of a distribution and its exponential transform. We will assume for this discussion that we are dealing with even, Gaussian-shaped distributions or their even approximations that are everywhere non-negative. If the distribution is continuous, then the variance is given by

$$\sigma^2 = \frac{\frac{d^2 H(s)}{ds^2} \Big|_{s=0}}{H(s=0)} = \frac{\int_{-\infty}^{+\infty} t^2 h(t) dt}{\int_{-\infty}^{+\infty} h(t) dt} \quad (38)$$

where $H(s)$ is the Laplace transform of $h(t)$. If the signal is discrete, then

$$\begin{aligned} \sigma^2 &= \frac{z^2 \frac{d^2 H(z)}{dz^2} \Big|_{z=1}}{H(z=1)} = \frac{\sum_{n=-\infty}^{n=+\infty} n(n+1)h[n]}{\sum_{n=-\infty}^{n=+\infty} h[n]} \\ &= \frac{\sum_{n=-\infty}^{n=+\infty} n^2 h[n]}{\sum_{n=-\infty}^{n=+\infty} h[n]} \end{aligned} \quad (39)$$

where $H(z)$ is the z -transform of $h[n]$. To treat the second moments as the variances of distributions, we have normalized (38) and (39) with $H(s=0)$ and $H(z=1)$ and used the assumption of an even distribution (e.g., $h[n] = h[-n]$), meaning that the average is zero.

Applying (38) to (4) implies that if we were implementing Gaussian filtering by differential equations and not difference equations, we would then have the result in [13], namely

$$\sigma^2 = \frac{2a_2}{a_0} q^2 = 1.17709q^2. \quad (40)$$

This is a clear indication that there is a deterministic transformation of the parameter q to the width σ . We are dealing, however, with difference equations that provide a recursive method to produce a Gaussian impulse response. Applying (39) to the product of (8) and (9) yields

$$\sigma^2 = -\frac{2(b_2 b_3 + b_1(b_2 + 4b_3) + b_0(b_1 + 4b_2 + 9b_3))}{(b_0 + b_1 + b_2 + b_3)^2} \quad (41)$$

where the \mathbf{b} coefficients are defined in (10). Substituting these values gives

$$\begin{aligned} \sigma^2 &= \frac{2(2m_0^2 m_1^2 + m_1^4 - 2m_0^2 m_2^2 + 2m_1^2 m_2^2 + m_2^4)}{m_0^2 (m_1^2 + m_2^2)^2} q^2 \\ &\quad + \frac{2(2m_0 m_1 + m_1^2 + m_2^2)}{m_0 (m_1^2 + m_2^2)} q. \end{aligned} \quad (42)$$

Equation (42) is quadratic in q , leading to a straightforward expression for determining q starting from σ . Before proceeding,

however, let us first examine the value of this expression for the specific values of \mathbf{m} given in (6). Substitution leads to

$$\sigma^2 = 1.17709q^2 + 3.09727q. \quad (43)$$

The first term is recognizable from (40) as being due to the polynomial approximation in (4). The second term in (43) (the term that is linear in q) is due to the finite difference approximation. At this point, we can solve the quadratic (43) to determine $q(\sigma)$, as given in (11). Considering the general case as defined in (42), however, allows us to develop an expression for $q(\sigma)$ that can be used with other optimization criteria that lead to another set \mathbf{m} .

To determine the required q corresponding to a desired σ , we use the standard quadratic equation $aq^2 + bq + c = 0$ and then write one of the solutions as

$$q = \frac{b}{2a} \left(\sqrt{1 - \frac{4ac}{b^2}} - 1 \right). \quad (44)$$

Mathematica [15] easily identifies the terms $\{a, b, c\}$ in (42), giving the general solution

$$\begin{aligned} \frac{b}{2a} &= \frac{m_0 (m_1^2 + m_2^2) (2m_0 m_1 + m_1^2 + m_2^2)}{2(2m_0^2 (m_1^2 - m_2^2) + (m_1^2 + m_2^2)^2)} \\ \frac{4ac}{b^2} &= -\frac{2(2m_0^2 (m_1^2 - m_2^2) + (m_1^2 + m_2^2)^2)}{(2m_0 m_1 + m_1^2 + m_2^2)^2} \sigma^2. \end{aligned} \quad (45)$$

The values of the coefficients \mathbf{m} are given in (6), and this gives, on substitution in (45)

$$\begin{aligned} \frac{b}{2a} &= 1.31564 \\ \frac{4ac}{b^2} &= -0.490811\sigma^2. \end{aligned} \quad (46)$$

This leads immediately to (11). Should we desire to use another optimization criterion to choose the set \mathbf{a} , then this will lead to another set \mathbf{m} and, eventually, to new values for (46).

ACKNOWLEDGMENT

The authors would like to thank Prof. A. Katsaggelos for his hospitality and the interaction with his group during the preparation of this manuscript at Northwestern University.

REFERENCES

- [1] D. Gabor, "Theory of communications," *Proc. Inst. Elect. Eng.*, vol. 93, pp. 429–459, 1946.
- [2] A. V. Oppenheim, A. S. Willsky, and I. T. Young, *Systems and Signals*. Englewood Cliffs, NJ: Prentice-Hall, 1983.
- [3] N. Petkov, "Image classification system based on cortical representation and unsupervised neural network learning," in *Proc. Conf. Comput. Archit. Machine Perception*, Pavia, Italy, 1995.
- [4] J. G. Daugman, "Uncertainty relations for resolution in space, spatial frequency, and orientation optimized by two-dimensional visual cortical filters," *J. Opt. Soc. Amer. A*, vol. 2, pp. 1160–1169, 1985.
- [5] J. P. Jones and L. A. Palmer, "An evaluation of the two-dimensional Gabor filter model of simple receptive fields in cat striate cortex," *J. Neurophysiol.*, vol. 58, pp. 1233–1258, 1987.
- [6] B. G. Cumming and A. J. P. Parker, "Responses of primary visual cortical neurons to binocular disparity without depth perception," *Nature*, vol. 389, pp. 280–283, 1997.

- [7] T. S. Lee, "Image representation using 2D Gabor wavelets," *IEEE Trans. Pattern Anal. Machine Intell.*, vol. 18, pp. 959–971, July 1996.
- [8] S. N. Baker, E. Olivier, and R. N. Lemon, "Coherent oscillations in monkey motor cortex and hand muscle EMG show task-dependent modulation," *J. Physiol.*, vol. 501, pp. 225–241, 1997.
- [9] T. T. Chinen and T. R. Reed, "A performance analysis of fast Gabor transform methods," *Graphical Models Image Process.*, vol. 59, pp. 117–127, 1997.
- [10] C. Richard and R. Lengelle, "Joint recursive processing of time-frequency representations and their modified version by the reassignment method," *Signal Process.*, vol. 60, pp. 163–179, 1997.
- [11] S. Qiu, F. Zhou, and P. E. Crandall, "Discrete Gabor transforms with complexity $O(N \log N)$," *Signal Process.*, vol. 77, pp. 159–170, 1999.
- [12] I. T. Young and L. J. Van Vliet, "Recursive implementation of the Gaussian filter," *Signal Process.*, vol. 44, pp. 139–151, 1995.
- [13] L. J. Van Vliet, I. T. Young, and P. W. Verbeek, "Recursive Gaussian derivative filters," in *Proc. 14th Int. Conf. Pattern Recogn.*, Brisbane, Australia, 1998.
- [14] M. Abramowitz and I. A. Stegun, *Handbook of Mathematical Functions*. New York: Dover, 1965.
- [15] S. Wolfram, *Mathematica, A System for Doing Mathematics by Computer*, Second ed. Redwood City, CA: Addison Wesley, 1991.



Ian T. Young (SM'96) received the B.S., M.Sc., and Ph.D. degrees, all in electrical engineering, from the Massachusetts Institute of Technology (MIT), Cambridge, in 1965, 1966, and 1969, respectively.

From 1969 to 1973, he was an Assistant Professor of electrical engineering and, from 1973 to 1979, an Associate Professor of Electrical Engineering at MIT. From 1978 to 1981, he was a Group leader for pattern recognition and image processing at the Biomedical Sciences Division of Lawrence Livermore National Laboratory, University of California, Livermore. In

December 1981, he was appointed Chaired Professor of Measurement Technology and Instrumentation Science at the Department of Applied Physics, Delft University of Technology, Delft, The Netherlands. In 1998, he was appointed Chairman of the Department of Applied Physics in Delft. In July, 2002 he was appointed Chairman of the newly formed Department of Imaging Science and Technology. He has also been a Visiting Professor at a number of universities in the United States, Europe, and Asia. He is on the editorial boards of a number of scientific journals, co-author of a standard textbook *Signals and System*, and co-author of a web-book *Image Processing Fundamentals*, which can be found at <http://www.ph.tn.tudelft.nl/Courses/FIP/noframes/fip.html>.

Dr. Young has received a number of awards, most recently, the Leermeeester Prize in 1999 from the Universiteitsfonds of the Delft University of Technology, Fellow of the International Association for Pattern Recognition (IAPR) in 2000, and the Distinguished Service Award of the International Society for Analytical Cytology (ISAC) in 2002.



Lucas J. van Vliet received the M.Sc. degree in applied physics in 1988 and the Ph.D. degree, cum laude, in 1993 from the Delft University of Technology (DUT), Delft, The Netherlands.

He is a full professor of multidimensional data analysis with the Faculty of Applied Sciences, DUT. His thesis entitled "Grey-scale measurements in multi-dimensional digitized images" presents novel methods for sampling-error-free measurements of geometric object features. He has worked on CCD sensor characterization, nonlinear image

restoration, and measurement problems in quantitative microscopy applied to molecular biology. His current research includes segmentation and analysis of objects, textures and structures in multidimensional digitized images using adaptive, tensor filtering and orientation space analysis, and the segmentation-free processing of spatio-temporal images [3-D (x, y, t) and 4-D (x, y, z, t)] for motion analysis and image registration. He is a co-author of the web book *Image Processing Fundamentals*, which can be found at <http://www.ph.tn.tudelft.nl/Courses/FIP/noframes/fip.html>.

Dr. van Vliet was awarded the fellowship of the Royal Netherlands Academy of Arts and Sciences (KNAW) in 1996.

Michael van Ginkel received the M.Sc. degree in applied physics from the Delft University of Technology, Delft, The Netherlands, in 1995 on the subject of image filtering using anisotropic diffusion. His Ph.D. thesis is entitled "Image analysis using orientation space based on steerable filters."

He is currently a post-doctoral researcher, working on measurement in and characterization of (food) microstructures using image analysis.